

Chapter VI

Comparison of several *in situ* flagellar motors

Gavin E. Murphy, Ariane Briegel, Zhuo Li, D. Prabha Dias,

Gregory P. Henderson, Bingni Wen, Grant J. Jensen

Abstract

The flagellar motor is a tiny nanomachine that can spin at speeds of 60 to 1000 Hz yet occupies a space boxed by a 50 to 70 nm sided cube. Most of our information of it either comes from reconstructions of the *in vitro* *Salmonella* basal body or traditional electron microscopy images of stained, sectioned, or frozen-etched cells: on one end, a high-resolution, 3-D structure of the basal body stripped from its context; and on the other end, low-resolution, 2-D structure-pieces taken from traumatized cells and fraught with artifacts. Filling this gap are cryoelectron reconstructions of *in situ* flagellar motors. From few particles, the *Vibrio cholerae* and *Caulobacter crescentus* motor structures are presented in 3-D and compared to the better resolved *Treponema primitia* and *Hylemonella gracilis* motors. The variability suggests that structures taken from other bacterial species may display more novel or unusual features.

Introduction

The flagellar motor is interesting not just to scientists but to the public as well, because its remarkable abilities and beautiful structural components inspire the question of design. Darwinian evolution's explanation that such pieces gradually took shape and gradually came together seems unlikely initially because the finished product is so perfect-looking[1]. Experts conflict over whether the flagellar motor came from the type III secretion system (T3SS), which it resembles, or vice versa. Perhaps the gradualist explanation seems insufficient because only two structures are often compared: *Salmonella*'s basal body and T3SS[2, 3]. The structure determination of *T. primitia*'s flagellar motor and that of others shows that the flagellar motor is different across

species[4]. Divergence, if not emergence, can be shown graphically by comparison.

Three-dimensional information is necessary to determine the true differences in structure.

Over the decades, traditional electron microscopists have extracted flagellar basal bodies from many organisms, displayed their best images and measured the heights and diameters of the salient motor components[5-16]. Their measurements are compiled in Table VI-1, along with the author's. The images suffer from variability of stain and their 2-D nature. The measurements are just estimates, and some stand out as unusually small or large.

Electron cryotomography is a better technique, because with several tilt series a reconstruction of several complete bacterial cells can be generated and, what is more, identical macromolecular machines—too labile to purify or crystallize—can be computationally-extracted and averaged together to produce a higher resolution structure. This has been done with reconstructions of *Vibrio cholerae* and *Caulobacter crescentus* obtained from lab coworkers.

Results

Five good motor particles were extracted from five reconstructions of *Caulobacter crescentus*, aligned and averaged. No symmetry was detectable in the stator region, but 12-fold symmetry was applied to boost the signal-to-noise ratio. The final structure is shown in Figure VI-1. The low density of many features is visible in Figure VI-1B, where the contours are incremented in units of 78% of the standard deviation, with the white contour representing three times the standard deviation. The red contour was chosen for the isosurfaces in Figures VI-1C–D.

VI-4

Instead of discrete stator studs, a ring of density was seen above the membrane over the C ring with a central diameter of 41 nm (“S” in Figure VI-1D). The outer diameter of the C ring (“C”) is 42 nm, which supports the identity of the stator ring, since it is expected and (so far) always seen by the author, that the stator studs are right above the C ring. The resolution is insufficient to separate the C ring from the membrane. The density below the rotor is noisier than *H. gracilis*’ but may contain an export (E) mass. The rotor (“R”) density is continuous with the stator and inner membrane (IM) densities so its size is not measurable. Delineating the P and L ring is difficult because their density is continuous with each other and the outer membrane (OM), but there is a narrower ring in the expected peptidoglycan layer under a wider membranous ring. This is similar to the single particle reconstruction of the *Caulobacter* basal body, whose P ring appears slightly narrower than the L ring[17]. The rod extends upwards past the OM because it must transit the proteinaceous S layer.

Four good motor particles were extracted from four reconstructions of *V. cholerae*, aligned and averaged. No stator density was present, but the reconstruction was 12-fold symmetrized to improve the signal-to-noise ratio. The final structure is shown in Figure VI-2. The contours of the structure are shown in Figure VI-2B, which show that the *V. cholerae* motors are more contrast-rich than *Caulobacter*’s. The contours are incremented in standard deviation units, with the white contour representing 3.5 times the standard deviation. The red contour was chosen for the isosurfaces in Figures VI-1C–D. The outer diameter of the C ring is 46 nm. The resolution is insufficient to separate the C ring from the membrane. Below the rotor are two connected densities. These resemble the TA ring and export mass of *H. gracilis* (Chapter

5). The rotor is embedded in the membrane, so its borders are indeterminable. The bushings of *V. cholerae* are unusual compared to other species'. Negatively-stained images of the *V. alginolyticus* basal body revealed that the two P and L rings are half as high (3 nm) as *Salmonella*'s and are positioned over a novel T ring 31 nm in diameter[18]. In the same paper, they identified the T ring as consisting of MotX and MotY. A similar umbrella-shaped overhang is present in *V. cholerae*, but its outer diameter is 38 nm. It has been labeled a T ring in Figure VI-2D. Also unusual is the depression in which the rings sit in the outer membrane (OM). This may be an artifact of the low sample size or perhaps the L ring is truly small in height and connects with a tiny fraction of the OM to produce such a depression.

Discussion

The four *in situ* flagellar motors are compared to the *Salmonella* basal body[3, 19-21] in Figure VI-3. Each one is different: either a new structure is present or their dimensions are wider or narrower than *Salmonella*. The general features are tabulated in Table VI-2. Where previous research has made measurements of the four species, they will be compared. The chief insight is that the motors will need to be classified into groups: some may have wide bowl rotors, others narrower disk rotors; some will have P and L rings, others P collars. More discoveries await.

The principle discovery is the stator region and its symmetry. With ECT, 16 stator studs were seen in *T. primitia*[4] and 11–13 in *H. gracilis*. With freeze-etch microscopy, the maximum number of studs was either 12 or 16. The average number of studs in *Aquaspirillum serpens* and *Streptococcus* was 15 and ranged between 14 to 16[6,

10]. *E. coli* had an average of 11 and a range between 10 and 12[10]. *Bacillus firmus* had an average of 9 and a maximum of 12[11], and *Salmonella* had about 12 also[12]. The central diameters of the ring of stators give us an idea of the arc length per stator unit. For *T.p.*, *H.g.*, and *C.c.*, the central diameters are approximately 61, 48–51 and 41 nm, respectively, varying by 10 nm around *H.g.* The arc length per stud, where known, is ~ 12 nm for *T.p.* and *H.g.* Each stator unit is made from a complex of 4 MotA proteins, each containing 4 transmembrane (TM) alpha helices, and 2 MotB proteins, each having 1 TM helix. If one assumes a transmembrane helix is 1 nm in width, and that the MotA/B complex is arranged as predicted[22], with the 4 transmembrane helices of MotA surrounding the two transmembrane helices of MotB, then the complex is about 6 nm in diameter. Estimates of the stator dimensions from negatively stained, freeze-etch images seem too narrow given *Salmonella*'s standard rotor diameter of 31 nm. The outer and inner diameters of the stator studs in *B. firmus*, *E. coli*, and *Streptococcus* were 33 and 23 nm, 34 and 20 nm, and 40 and 26 nm, respectively[10, 11]. The inner diameter of the stator studs in *Salmonella* was 28 nm[12]. The dimensions of the stator studs should conform to the rough dimensions of the two OmpA domains of MotB. The height and girth of the studs were measured in *T.p.* and *H.g.* to be 9 and 7 nm, and 8 and 5 nm, respectively. Compared to the volume two OmpA domains, the *T.p.* stud volume was twenty times larger, but *H.g.*'s was approximately equal. They were 7 nm in girth in *B. firmus*, *E. coli*. and *Streptococcus* and 5 nm in *A. serpens*[6, 10, 11].

The *T.p.* stators are the most unusual. Their studs have connecting density between them and the presence of the P collar on the stators might suggest that all are needed to be present to support the P collar. This does not seem likely though, as

functional studies of *E. coli* and *Streptococcus* motors have proven that a full-complement of stators is not required to turn the rotor[23], and the number of stator studs in freeze-etch images even varies between motors within the same cell. Another oddity of *T.p.* is that the MotA/B complex is expected to be 2-fold symmetric[22], but the connecting, finger-like density between the stators and the top rim of the rotor is not, or else such density would be visible on the outer diameter of the studs. This suggests there are unknown adaptor proteins between the stators and the rotor, which might also serve to connect the P collar and stators.

In all reconstructions there is either symmetric or continuous connecting density between the C ring and the stator region of the IM. Three of the *in situ* motors had C ring diameters near *Salmonella*'s except *T.p.*, which had a 64 nm wide C ring. The C rings extended about 15–20 nm into the cytoplasm from the IM.

A dense structure labeled an export mass is present below the rotor in all structures and may be a ribosome feeding flagellin monomers through either a transport apparatus (TA) ring present in nearly all structures or perhaps through the rotor. In older EM images, “insertion pores” were seen under the rotor with a diameter of ~ 10 nm in *Caulobacter*, *Salmonella*, and *Spirochaeta aurantia* rotors[17, 24, 25]. The TA rings in *T.p.* and *H.g.* are wider, at ~ 20 nm.

The rotor is embedded in the IM and so its borders are indistinguishable except in *T.p.* There are two clear rims that may correspond to the membrane (M) and supermembranous (S) rings. It is unclear whether the stators in narrower motors also have connecting density to the rotor. The chief difference in rotors is the wide bowl rotor in *T.p.* and the normal-sized, disk rotors in everything else. *T. primitia*'s top rim diameter

of 24 nm is comparable to the S ring values in other organisms, but its bottom rim is much wider, at 38 nm. In *Salmonella* and *Caulobacter* reconstructions, the M and S rings have diameters of 26.5 and 27.5 nm, and 24 and 28 nm, respectively[17, 26]. In 2D EM images of the basal bodies in *A. serpens*, *Campylobacter fetus*, *Wolinella succinogenes*, and *E. coli*, the M and S rings have diameters of 31 and 28 nm, 26 and 26 nm, 30 and 30 nm, and 22.5 and 22.5 nm, respectively[6, 10, 14]. One unexpected discovery is the distance between the C ring and rotor in *in situ* versus *in vitro* reconstructions. There is no visible connecting density even in the higher-resolution *in vitro* reconstruction, and the gap is ~ 2 nm[3]. See the star and tethers drawn in Figure VI-3. In *H.g.* and *T.p.* the gap is ~ 3 times longer, so whatever tether connects them must be stretched in the *in situ* motor.

Another difference resides in the peptidoglycan and outer membrane bushings: the P and L rings. Although their density is continuous with each other and the OM, the general outline reveals small differences between the gram negative bacteria, and large differences between them and *T.p.* In *C.c.*, the L ring is wider than the P ring in both the *in situ* reconstruction and the *in vitro* one[17]. The L and P rings in *Vibrio* are thinner, and underneath them is an overhanging T ring[18]. In *H.g.*, the P ring appears to be supplemented with an extended E collar. The biggest difference is the P collar in *T.p.* The presence of a P collar instead of a P ring is a manifestation of the lack of FlgI in the genomes of *Treponema*, but the gene responsible for the P collar is unknown[27]. The P ring would restrict the tilt of the flagellum rod to a nearly vertical orientation, but the P collar would permit a wider range of bending of the rod and hook. In addition to genetic evidence, there are two images of *Spirochaeta stenostrepta* insertion pores which show a

shape resembling a P collar[7]. Interestingly, Firmicutes also lack FlgI, so it is tempting to speculate that Firmicutes have a P collar also. Since the P collar is twice as high as *Salmonella*'s P ring, maybe the P collar would suffice to create a pore opening in the thicker peptidoglycan layer of gram positive bacteria.

The motors probably do not partition into two neat categories with wide rotors and P collars or narrow rotors and P rings. *Borrelia* and *Leptospira* both appear to have wide rotors in EM images but both have the P ring gene[27]. Curiously, *Leptospira* also has an L ring gene even though its flagella never exit the periplasm. It may be that there are a wide variety of motor attachments and component versions present in the bacterial world.

Methods

Image processing was carried out as described before[4].

References

1. Pallen, M. J., and Matzke, N. J. From The Origin of Species to the origin of bacterial flagella. *Nat Rev Microbiol.* **4**, 784-90 (2006).
2. Marlovits, T. C., et al. Structural insights into the assembly of the type III secretion needle complex. *Science.* **306**, 1040-2 (2004).
3. Thomas, D. R., Francis, N. R., Xu, C., and DeRosier, D. J. The three-dimensional structure of the flagellar rotor from a clockwise-locked mutant of *Salmonella enterica* serovar Typhimurium. *J Bacteriol.* **188**, 7039-48 (2006).

4. Murphy, G. E., Leadbetter, J. R., and Jensen, G. J. In situ structure of the complete *Treponema primitia* flagellar motor. *Nature*. **442**, 1062-4 (2006).
5. Abram, D., Vatter, A. E., and Koffler, H. Attachment and structural features of flagella of certain bacilli. *J Bacteriol.* **91**, 2045-68 (1966).
6. Coulton, J. W., and Murray, R. G. Cell envelope associations of *Aquaspirillum serpens* flagella. *J Bacteriol.* **136**, 1037-49 (1978).
7. Holt, S. C., and Canale-Parola, E. Fine structure of *Spirochaeta stenostrepta*, a free-living, anaerobic spirochete. *J Bacteriol.* **96**, 822-35 (1968).
8. Hovind-Hougen, K., Birch-Andersen, A., and Jensen, H. J. Ultrastructure of cells of *Treponema pertenu* obtained from experimentally infected hamsters. *Acta Pathol Microbiol Scand [B]*. **84**, 101-8 (1976).
9. Jackson, S., and Black, S. H. Ultrastructure of *Treponema pallidum* Nichols following lysis by physical and chemical methods. II. Axial filaments. *Arch Mikrobiol.* **76**, 325-40 (1971).
10. Khan, S., Dapice, M., and Reese, T. S. Effects of *mot* gene expression on the structure of the flagellar motor. *J Mol Biol.* **202**, 575-84 (1988).
11. Khan, S., Ivey, D. M., and Krulwich, T. A. Membrane ultrastructure of alkaliphilic *Bacillus* species studied by rapid-freeze electron microscopy. *J Bacteriol.* **174**, 5123-6 (1992).
12. Khan, S., Khan, I. H., and Reese, T. S. New structural features of the flagellar base in *Salmonella typhimurium* revealed by rapid-freeze electron microscopy. *J Bacteriol.* **173**, 2888-96 (1991).

13. Khan, S., Zhao, R. B., and Reese, T. S. Architectural features of the Salmonella typhimurium flagellar motor switch revealed by disrupted C-rings. *Journal Of Structural Biology*. **122**, 311-319 (1998).
14. Kupper, J., Wildhaber, I., Gao, Z., and Baeuerlein, E. Basal-body-associated disks are additional structural elements of the flagellar apparatus isolated from *Wolinella succinogenes*. *J Bacteriol*. **171**, 2803-10 (1989).
15. Nauman, R. K., Holt, S. C., and Cox, C. D. Purification, ultrastructure, and composition of axial filaments from *Leptospira*. *J Bacteriol*. **98**, 264-80 (1969).
16. Paster, B. J., and Canale-Parola, E. Involvement of periplasmic fibrils in motility of spirochetes. *J Bacteriol*. **141**, 359-64 (1980).
17. Stallmeyer, M. J., Hahnenberger, K. M., Sosinsky, G. E., Shapiro, L., and DeRosier, D. J. Image reconstruction of the flagellar basal body of *Caulobacter crescentus*. *J Mol Biol*. **205**, 511-8 (1989).
18. Terashima, H., Fukuoka, H., Yakushi, T., Kojima, S., and Homma, M. The Vibrio motor proteins, MotX and MotY, are associated with the basal body of Na-driven flagella and required for stator formation. *Mol Microbiol*. **62**, 1170-80 (2006).
19. Francis, N. R., Sosinsky, G. E., Thomas, D., and DeRosier, D. J. Isolation, characterization and structure of bacterial flagellar motors containing the switch complex. *J Mol Biol*. **235**, 1261-70 (1994).
20. Thomas, D., Morgan, D. G., and DeRosier, D. J. Structures of bacterial flagellar motors from two FliF-FliG gene fusion mutants. *J Bacteriol*. **183**, 6404-12 (2001).

21. Thomas, D. R., Morgan, D. G., and DeRosier, D. J. Rotational symmetry of the C ring and a mechanism for the flagellar rotary motor. *Proc Natl Acad Sci U S A*. **96**, 10134-9 (1999).
22. Braun, T. F., Al-Mawsawi, L. Q., Kojima, S., and Blair, D. F. Arrangement of core membrane segments in the MotA/MotB proton-channel complex of *Escherichia coli*. *Biochemistry*. **43**, 35-45 (2004).
23. Berg, H. C. The rotary motor of bacterial flagella. *Annu Rev Biochem*. **72**, 19-54 (2003).
24. Katayama, E., Shiraishi, T., Oosawa, K., Baba, N., and Aizawa, S. Geometry of the flagellar motor in the cytoplasmic membrane of *Salmonella typhimurium* as determined by stereo-photogrammetry of quick-freeze deep-etch replica images. *J Mol Biol*. **255**, 458-75 (1996).
25. Brahamsha, B., and Greenberg, E. P. Biochemical and cytological analysis of the complex periplasmic flagella from *Spirochaeta aurantia*. *J Bacteriol*. **170**, 4023-32 (1988).
26. Sosinsky, G. E., Francis, N. R., Stallmeyer, M. J., and DeRosier, D. J. Substructure of the flagellar basal body of *Salmonella typhimurium*. *J Mol Biol*. **223**, 171-84 (1992).
27. Pallen, M. J., Penn, C. W., and Chaudhuri, R. R. Bacterial flagellar diversity in the post-genomic era. *Trends Microbiol*. **13**, 143-9 (2005).

Author Contributions G.E.M. collected some data, analyzed all the data, and drafted the text and figures. A.B., Z.L., D.P.D., G.P.H. and B.W. provided most of the data. G.J.J supervised all the work.

Figures

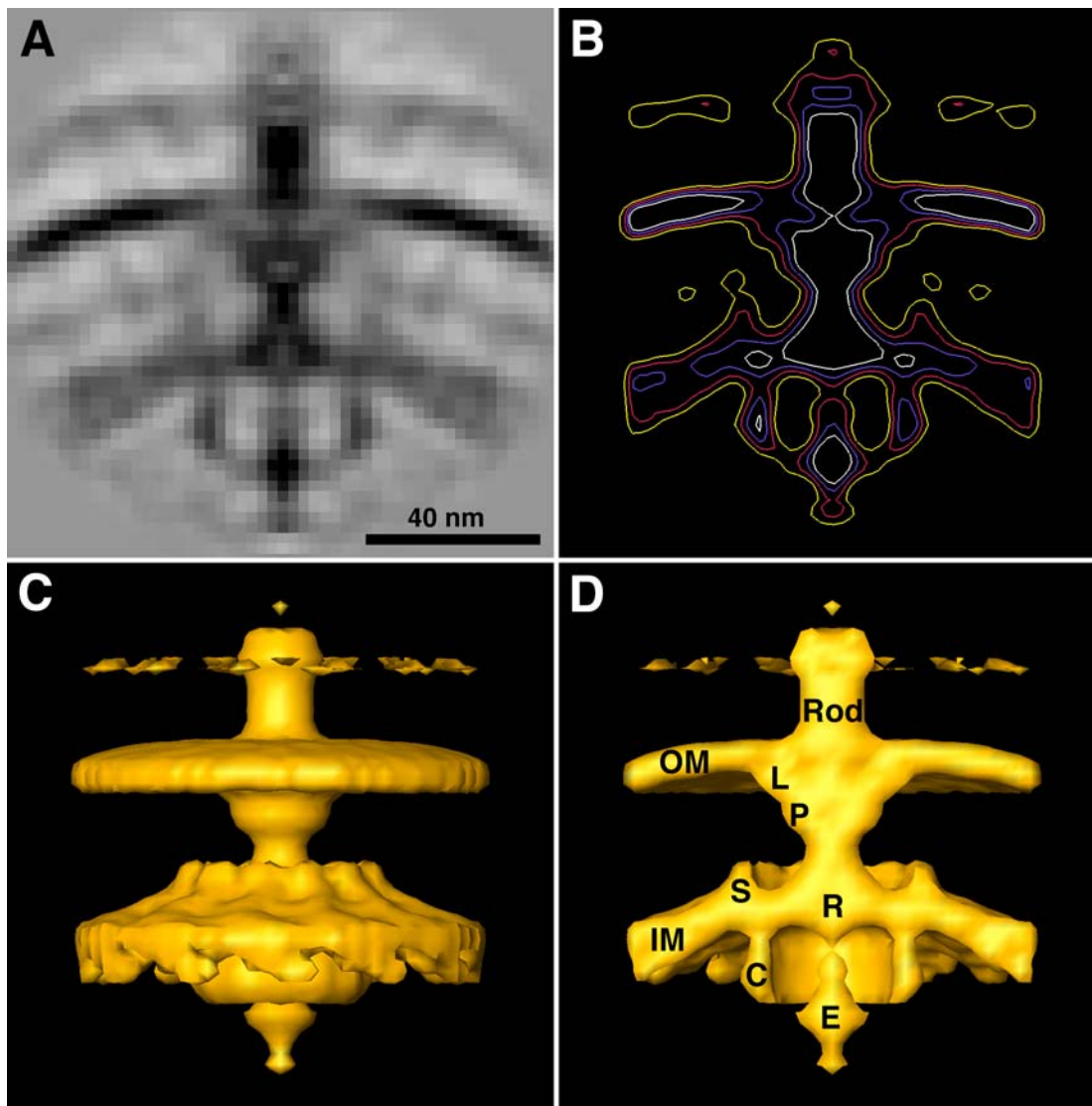


Figure VI-1. *Caulobacter crescentus* flagellar motor

A. 2.4 nm-thick axial section through the 12-fold symmetrized motor. B. Contours through the symmetrized motor. The red contour was chosen for isosurfacing. C. Side view isosurface of the motor. D. Cutaway of the motor.

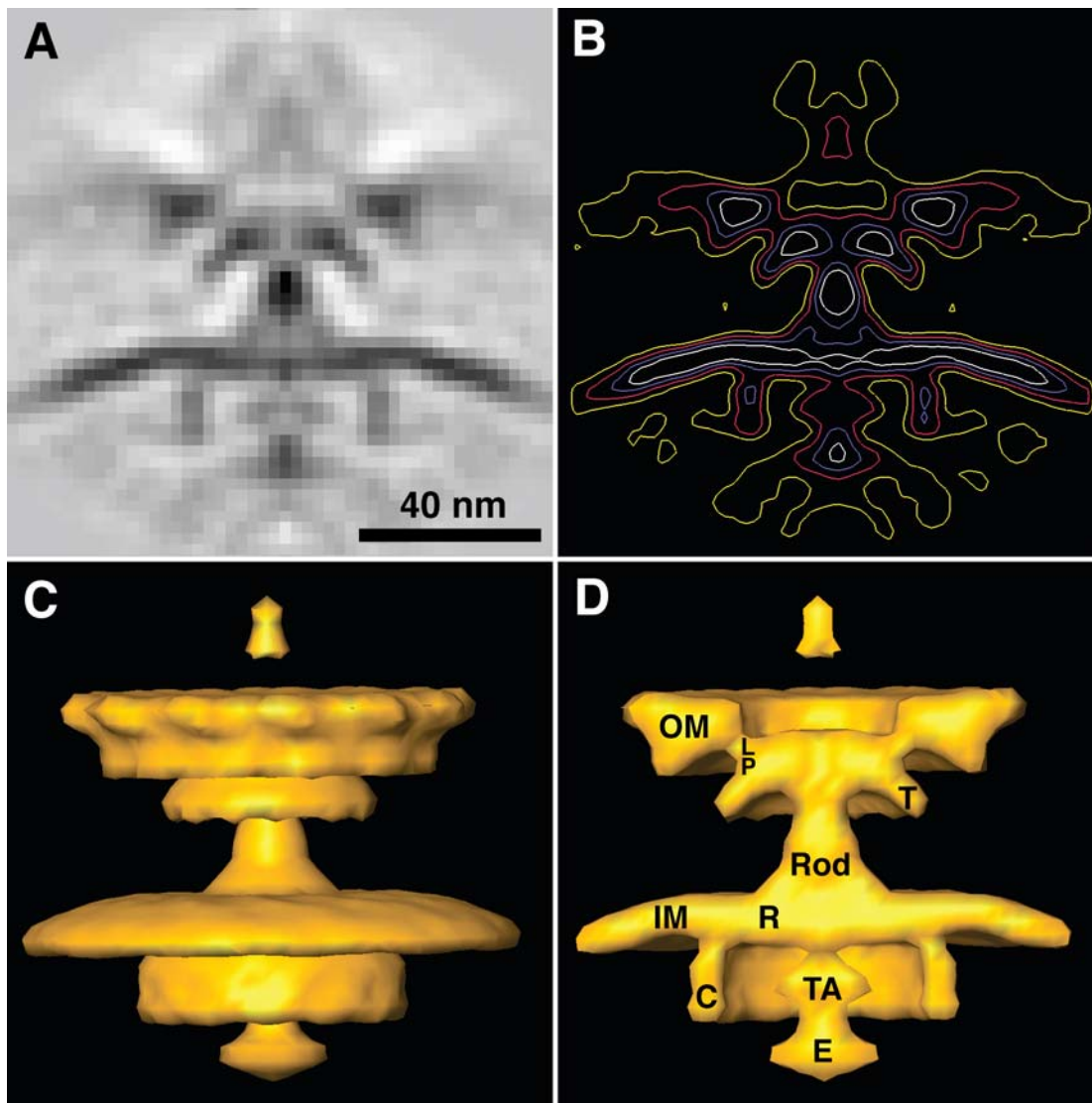


Figure VI-2. *Vibrio cholerae* flagellar motor

- A. 2.4 nm-thick axial section through the 12-fold symmetrized flagellar motor. B. Contours through the symmetrized motor. The red contour was chosen for isosurfacing. C. Side view isosurface of the motor. D. Cutaway of the motor.

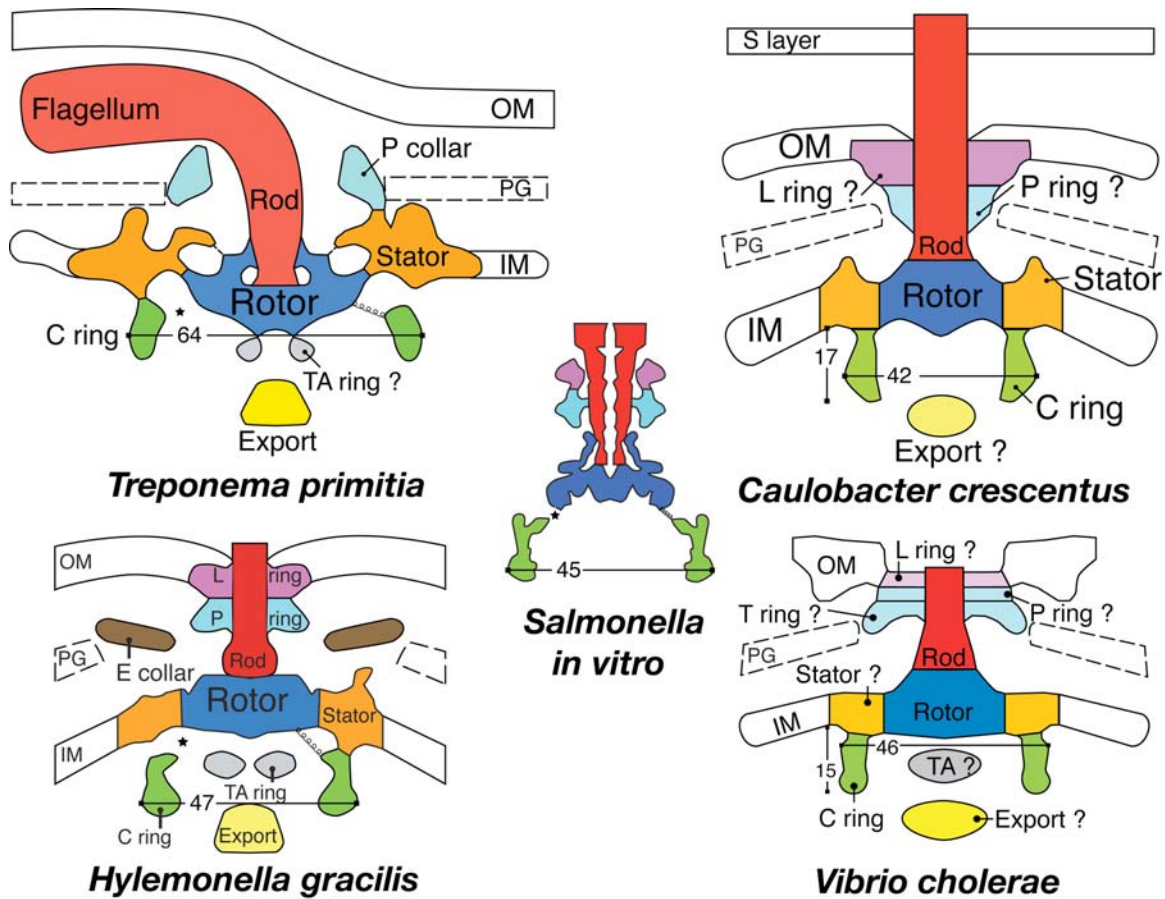


Figure VI-3. *In situ* flagellar motors in comparison to *Salmonella in vitro*

All motors are approximately to scale. Stator studs are visible in all except *V. cholerae*. All motors have high-contrast density below their rotor that has been labeled as Export and may be a ribosome feeding monomers through the rotor. A ring labeled as a transport apparatus (TA) ring exists below *T. primitia* and *H. gracilis*, and may exist below *V. cholerae*. The L ring, P ring, and rotor borders were drawn by consulting the dimensions of negatively stained *in vitro* images of the respective motors, except for *H. gracilis*. The L ring, P ring, rotor, and stator densities are often continuous with the membranes and thus difficult to delineate.

Phylum	Name	Rod	L-ring	P-ring	P-collar	S-ring	M-ring	Insertion Disk	Rotor shape	C-ring	Insertion Pore	Stator Number	stators	stud width	Ref
Proteobacteria beta	<i>H. gracilis</i> Height			7											
	<i>H. gracilis</i> Diameter	12		26	24				disk	47		11-13	center 48-51	5	Murphy, unpublished
	<i>Aquaspirillum</i>			21	28	31						16 max		5	Coulton, 1978
	<i>beta serpens</i>			21	28	31						16 max		5	Coulton, 1978
alpha	Caulobacter Height		31 or										center 41		Stallmeyer 1989
	Caulobacter Diam		34	25	24	28			disk	42 (Murphy)	10 (outer)		center 41 (Murphy)		Murphy, unpublished
gamma	<i>Salmonella</i> Height	21	16 / 2	16 / 2							5				1994 did Cring into; Thomas 2006 best for S;
						3.5 or 5; 2.7 best	6.5				17				Khan, 1991 did stators; Sosinsky 1992 did rotor; Francis 1994 did C ring; Katayama 1996 did pore; Thomas 2006 best for M,S rings
gamma	<i>Salmonella</i> Diam	11.5	26	27.5	24	29			disk	45 (outer); 47-49 Thomas 2006	9 (outer)	12 max	22 or 28 int. diam.		Khan, 1991 did stators; Sosinsky 1992 did rotor; Francis 1994 did C ring; Katayama 1996 did pore; Thomas 2006 best for M,S rings
gamma	<i>Ectothiorhodospira mobilis</i>	6	25	25	20-25	20-25									Kupper 1989
gamma	<i>E. coli</i>	8.5, 7	22.5	22.5	22.5	22.5						12 max	20 (inner), 34 (outer)	7	Khan Dapice 1988; Kupper 1989 for rings and value "7" for Rod Kupper 1989; Murphy, unpublished
gamma	<i>Vibrio cholerae</i>	8	23	23	11	11			disk	46 (Murphy)					Kupper 1989
epsilon	<i>Campylobacter fetus</i>		39	39	26	26									Kupper 1989
epsilon	<i>Wolinella succinogenes</i>	13	30	30	30	30									Kupper 1989
Firmicutes	<i>Streptococcus</i>	10													Kupper 1989
	<i>Bacillus firmus</i>														Kupper 1989
	<i>Bacillus</i>														Kupper 1989
	<i>stearothermophilus</i>		no	no											Khan Dapice 1988
	<i>Bacillus brevis</i>								mushroom or disk			16 max	26 (inner), 40 (outer)	7	Khan Dapice 1988
Spirochaetes	<i>Bacillus</i>														Khan, Ivey 1992
	<i>T. primitia</i> Height		no	no	15 ~4 (outer), 28 (inner)	24	38								Abram Vatter 1966
	<i>T. primitia</i> Diameter	12	no	no							5				Abram Vatter 1966
	<i>Spirochaeta aurantia</i>	12	no	no											Abram Vatter 1966
	<i>Leptospira interrogans</i>		yes	yes				40 to 45	mushroom or disk shaped; has a button						Brahamsha 1988
	<i>Spirochaeta halophila</i>		no	no				40 or 42 *	mushroom						Nauman 1969
	<i>Spirochaeta stenostrepta</i>		no	no				40 to 45	mushroom						Paster 1980
	<i>Treponema pallidum</i>	12 to 13	no	no				supposedly 60, probably more like 40 or 50; also 30-35	39						Holt Canale-Parola 1969
	<i>Borrelia recurrentis</i>		no	no				30 to 35	mushroom or disk						Jackson 1971; 30-35 comes from Holt 1978
	<i>Borrelia burgdorferi</i>		no	gene				30 to 35							Holt 1978
	<i>Borrelia garinii</i>		no	gene				30 to 35							blast
	<i>Brachyspira aalborgi</i>		no	gene				33	disk						blast
	<i>Brachyspira</i> env. sample		no	no				40 *	disk						Hovind-Hougen 1982
									disk						Tasu 2003

Table VI-1. Flagellar motor measurements

Starred measurements were measured from the papers' figures and scale bars.

	Rotor	Stator	C ring	P bushing	L ring	Export	TA ring	Extra?
<i>Salmonella</i>	Normal	Normal 12	Normal	Ring	Yes	-	-	-
<i>T. primitia</i>	Wide	Wide	Wide	Collar	No	Yes	Probably	P Collar
<i>H. gracilis</i>	Normal ?	Normal 11-13	Normal	Ring, wider than <i>Sal</i>	Probably	Yes	Yes	E collar
<i>V. cholerae</i>	Normal ?	-	Normal	Ring ?	Probably	Yes	Maybe	T ring
<i>C. crescentus</i>	Normal ?	Narrow	Narrow	Ring ?	Probably	Maybe	-	S layer

Table VI-2. Motor components in the five structures